Direct Comparison between Potential Landscape and Local Density of States in a Disordered Two-Dimensional Electron System

M. Morgenstern,[1] J. Klijn,[1] Chr. Meyer,[1] M. Getzlaff,[1] R. Adelung,[2] R. A. Römer,[3] K. Rossnagel,[2]
L. Kipp,[2] M. Skibowski,[2] and R. Wiesendanger[1]

[1]*Institute of Applied Physics, Hamburg University, Jungiusstraße 11, D-20355 Hamburg, Germany*
[2]*Institute for Experimental and Applied Physics, Christian-Albrechts-University Kiel, Leibnizstraße 19, D-24098 Kiel, Germany*
[3]*Institute of Physics, Chemnitz University of Technology, 09107 Chemnitz, Germany*

The local density of states (LDOS) of the adsorbate-induced two-dimensional electron system (2DES) on n-InAs(110) is studied by scanning tunneling spectroscopy. In contrast to a similar 3DES, the 2DES LDOS exhibits 20 times stronger corrugations and rather irregular structures. Both results are interpreted as consequences of weak localization. Fourier transforms of the LDOS reveal that the k values of the unperturbed 2DES still dominate the 2DES, but additional lower k values contribute. To clarify the origin of the LDOS patterns, we measure the potential landscape of the 2DES area. We use it to calculate the expected LDOS and find reasonable agreement between calculation and experiment.

Two-dimensional electron systems (2DES) in semiconductors are intensively studied as a paradigmatic case for many-particle systems in disordered potentials [1]. They exhibit unique properties with respect to their three-dimensional counterparts such as weak localization or the quantum Hall effect [2]. Many experiments probed their macroscopic properties leading to detailed predictions for the local density of states (LDOS) [2,3], but this LDOS has never been probed directly. Consequently, LDOS studies on a semiconductor 2DES are highly desirable [4,5]. We use the adsorbate-induced 2DES on InAs(110) [6] to record the 2DES LDOS by scanning tunneling spectroscopy (STS). A spatial resolution of 5 nm is achieved well below characteristic length scales of the 2DES [7]. We found that the well-known tendency of a 2DES to weakly localize results in strong and irregular LDOS corrugations in remarkable contrast to 3DES's, where only weak and regular corrugations are found [8]. Moreover, the main features of the 2DES LDOS are reproduced by solving the corresponding single-particle Schrödinger equation (SE).

The UHV-low temperature STM working at $T = 6$ K with spectral resolution in STS down to 1 mV is described elsewhere [9]. Degenerate n-InAs ($N_D = 1.1 \times 10^{16}/\text{cm}^3$) is cleaved *in situ* at a base pressure of 10^{-8} Pa, which leads to a nearly defect free InAs(110) surface with a Fermi level $E_F = 5$ meV above the conduction band minimum. To induce the 2DES, Fe is deposited from an e-beam evaporator [6]. The Fe coverage is determined by counting the Fe atoms and given with respect to the unit cell of InAs(110). Topographic STM images are recorded in constant current mode with voltage V applied to the sample. The dI/dV curves are measured by lock-in technique ($f = 1.5$ kHz, $V_{\text{mod}} = 1.8$ mV) with fixed tip-surface distance stabilized at current I_{stab} and voltage V_{stab}. The $dI/dV(V)$ images are measured point by point, each changing the voltage to V after stabilizing the tip at V_{stab} and I_{stab}. The influence of the spatially changing tip-surface distance is checked to be of minor importance [8]. Angle-resolved ultraviolet photoemission spectroscopy (ARUPS) experiments are performed on identically prepared samples using the HONORMI beam line at HASYLAB with photon energy $h\nu = 10$ eV and an ASPHERE analyzer. The total energy resolution was 20 meV and the angular resolution 0.25° in one and 0.45° in the other direction [10]. The Fermi level is determined on a clean Ta foil with an accuracy of 5 meV. The Fe flux is calibrated by a quartz balance.

Since a perturbing influence of the STM tip on the LDOS data cannot be excluded in STS on semiconductors [11], we determine the subband energies of the 2DES independently by ARUPS. Previous ARUPS measurements revealed the coverage dependence of the adsorbate-induced band shift and a rough estimate of the 2DES subband energies E_n [6]. With the high resolution of the ASPHERE analyzer, individual subband peaks are resolved [Fig. 1(a), points]. A straightforward fit of the data with the E_n's as the only fitting parameters [6] leads to $E_1 = -105 \pm 5$ meV and $E_2 = -40 \pm 5$ meV [see lines in Fig. 1(a)]. The resulting E_n's are additionally validated by measuring the angular dependence of the 2DES peak and fitting the data with the same procedure (not shown).

Next, we compare the ARUPS data with STS. Figures 1(b) and 1(d) show spatially averaged dI/dV curves representing the macroscopic average of the LDOS: the DOS [12]. The curves in Fig. 1(b) are measured with the same microtip before and after Fe deposition. Without Fe, two peaks caused by the tip induced quantum dot (QD) appear [11]. With Fe, the lower peak shifts to lower energy while the other disappears. The shift of the lower peak is caused by the
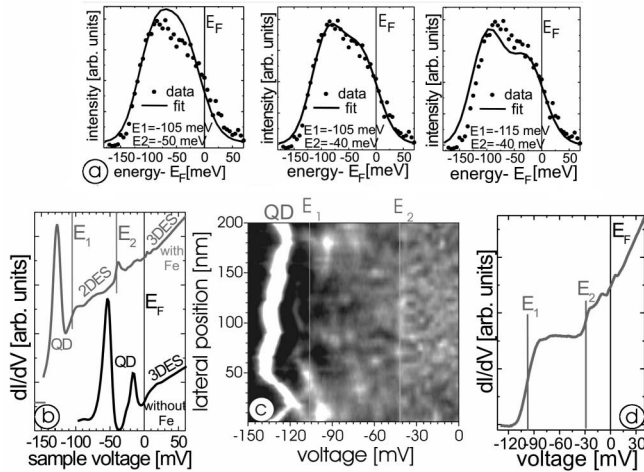
FIG. 1. (a) ARUPS spectrum of 4.5% Fe/n-InAs(110), $h\nu = 10$ eV (points) compared with fits for different subband energies E_1, E_2 as indicated (lines). Only the central curve fits the data. (b) Spatially averaged $dI/dV(V)$ curves of n-InAs(110) (lower curve) and 4.5% Fe/n-InAs(110) (upper curve); both curves taken with the same tip, $V_{stab} = 100$ mV, $I_{stab} = 500$ pA; peaks of the tip-induced quantum dot (QD) and E_1, E_2 of the 2DES determined by ARUPS as well as the 3DES are indicated. (c) Grey scale plot of $dI/dV(V)$ intensity as a function of position along a scan line, $V_{stab} = 100$ mV, $I_{stab} = 500$ pA; sample and tip as in upper curve of (b); E_1, E_2 and QD peak are indicated. (d) Spatially averaged $dI/dV(V)$ curve of 2.7% Fe/n-InAs(110), $V_{stab} = 100$ mV, $I_{stab} = 300$ pA; note the absence of QD peaks.

adsorbate-induced band bending. Indeed, the surface band shift of 300 meV measured by ARUPS requires a peak shift of 80 meV as evidenced by solving an equivalent of the Poisson-Schrödinger equation [6,11]. The disappearance of the second peak is caused by the reduction of the QD size due to the screening by the 2DES.

Between the QD peak and E_F, a rather flat dI/dV intensity with two steplike features at -108 and -43 mV is found. Since the features are located at the E_n's determined by ARUPS, we identify them with E_1 and E_2 of the 2DES. Additional evidence comes from Fig. 1(c), a grey scale plot of $dI/dV(V)$ along a substrate line. The 2DES region exhibits intensity fluctuations with a fluctuation length decreasing abruptly at E_2. This result is straightforwardly explained by the fact that the DOS doubles at E_2. Since each state has a different spatial phase, the fluctuation length of the LDOS decreases, although the fluctuation length of the second subband states is larger than the fluctuation length of the first subband states contributing at this energy.

Figure 1(d) shows another spatially averaged dI/dV curve recorded with a different tip at slightly lower Fe coverage. E_n's as determined from ARUPS are marked again. The QD states are absent and clear steplike structures as expected from a 2DES DOS are visible at the E_n's. We conclude that the presence of the QD does not change the energies in the steplike DOS, but slightly influences the intensity distribution.

The presence of the QD provides a unique advantage. As described elsewhere, the energy of the lowest QD state follows the electrostatic potential in the center of the QD [11]. Since the extension of the QD state perpendicular to the surface is the same as the extension of the 2DES, the QD state directly monitors the local 2DES potential. Indeed, the QD energy fluctuates with position as visible in Fig. 1(c) (curved line along the y axis at QD). A plot of the QD energy as a function of position is shown in Fig. 2(a). Four dominant troughs about 20 meV in depth are visible. This is exactly the number of substrate donors on average located within the 2DES area and exactly the attractive potential of a single donor averaged over the extension of the 2DES. We take both as strong evidence that the QD state indeed maps the 2DES potential. Additional smaller troughs are visible, which are attributed to donors further away from the 2DES.

What is the influence of the Fe atoms? An STM image of a small area of Fig. 2(a) (black square) is given in Fig. 2(b). It shows several Fe atoms (dark dots), but no correspondence between the Fe positions and the measured potential. This might be surprising, since the adsorbate layer donates electrons to the 2DES and is thus charged [6]. Anyway, in the area of Fig. 2(a) only 700 electrons are donated [13], but 7000 Fe atoms (4.5% coverage) are deposited. Since each Fe atom provides one electron at E_F, an electron density of 1.5×10^{13} cm^{-2} remains in the Fe layer sufficient to screen the positive charge on small length scales.

Figure 2(c) shows a more irregular potential obtained at 0.8% coverage. It exhibits more troughs than expected from the 16 bulk donors. Here, the remaining electron density in the Fe layer of 2×10^{12}/cm^{-2} is not sufficient to screen the positive charge of $8 \times 10^{11} e$/cm^{-2} completely. The measured potential can be used to estimate the mean free path in the 2DES. Using a reasonable scattering cross section of 10 nm^2 per dopant [8,14], it turns out to be about 3 μm for Fig. 2(a). This value is lower but already comparable to high-mobility 2DES's stressing the relevance of the STS results for transport measurements.
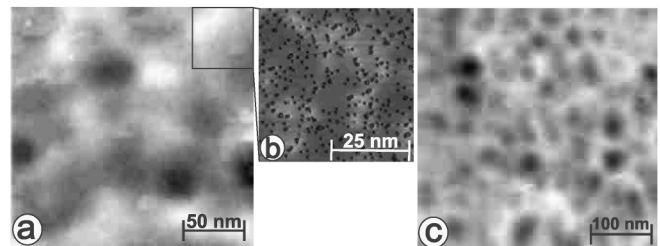

FIG. 2. (a) Potential landscape as determined from laterally fluctuating peak voltage of the lowest-energy QD state, 4.5% Fe/n-InAs(110). (b) Constant-current image of the area marked in (a) $V = 100$ mV, $I = 50$ pA; dark spots are Fe atoms. (c) Potential landscape at 0.8% Fe/n-InAs(110). Both potential images cover a potential range of 20 meV.

Next, we discuss the LDOS. Figures 3(a)–3(g) show some of the LDOS images recorded at 2.7% coverage in the absence of a QD. The spatial resolution is 5 nm well below the Fermi wave length of 23 nm. The total intensity in each image corresponds on average to 30 electronic states [15], but, since the scattering length and thus the localization length is larger than the image size, more states contribute with part of its intensity. The LDOS images exhibit corrugations decreasing in length scale with increasing V. The corrugation patterns are rather complicated and do not exhibit the circular structures found in the InAs 3DES [8]. The corrugation strength defined as the ratio between spatially fluctuating and total dI/dV intensity is 60% ± 5%, i.e., 20 times larger than the corrugation strength in the 3DES (3% ± 0.5%) [8]. Both results reflect the tendency of the 2DES to weakly localize [2]. Many different scattering paths, each containing many scattering events, contribute to the LDOS leading to more intricate patterns, and the tendency for localization leads to the increased corrugation. Notice that 2DES and 3DES are derived from the same conduction band, are measured at the same kinetic energy, and the strength of the potential disorder is the same. Consequently, the comparison between 3DES and 2DES

is direct and the strong differences underline the importance of dimensionality in the interaction of electronic states with potential disorder as early pointed out by Anderson [2].

Fourier transforms (FT's) of the LDOS (insets) reveal the distribution of contributing k values. At low voltage a disk is visible in the FT, which at higher voltage is confined by a ring. At even higher voltages ($V > -40$ mV), a second smaller disk appears, indicating the occupation of the second subband. A plot of the k values corresponding to the rings is shown in Fig. 3(h). At low voltages, where the ring is not apparent, the outer diameter of the disk is taken. For comparison, the $E(k)$ dispersion of unperturbed InAs [16] is drawn. The correspondence of the dispersion curve with the data is excellent for the lower subband and slightly worse for the second subband, demonstrating that the unperturbed k values still dominate the spectrum. However, additional k-space intensity within the rings is found in the FT's [17].

For 0.8% coverage [Figs. 3(i)–3(l)], we find the same tendencies as for 2.7% coverage. Here, only one subband is occupied ($E_1 = -60$ meV) and the tip exhibits a QD state. From the QD state, the potential in Fig. 2(c) results
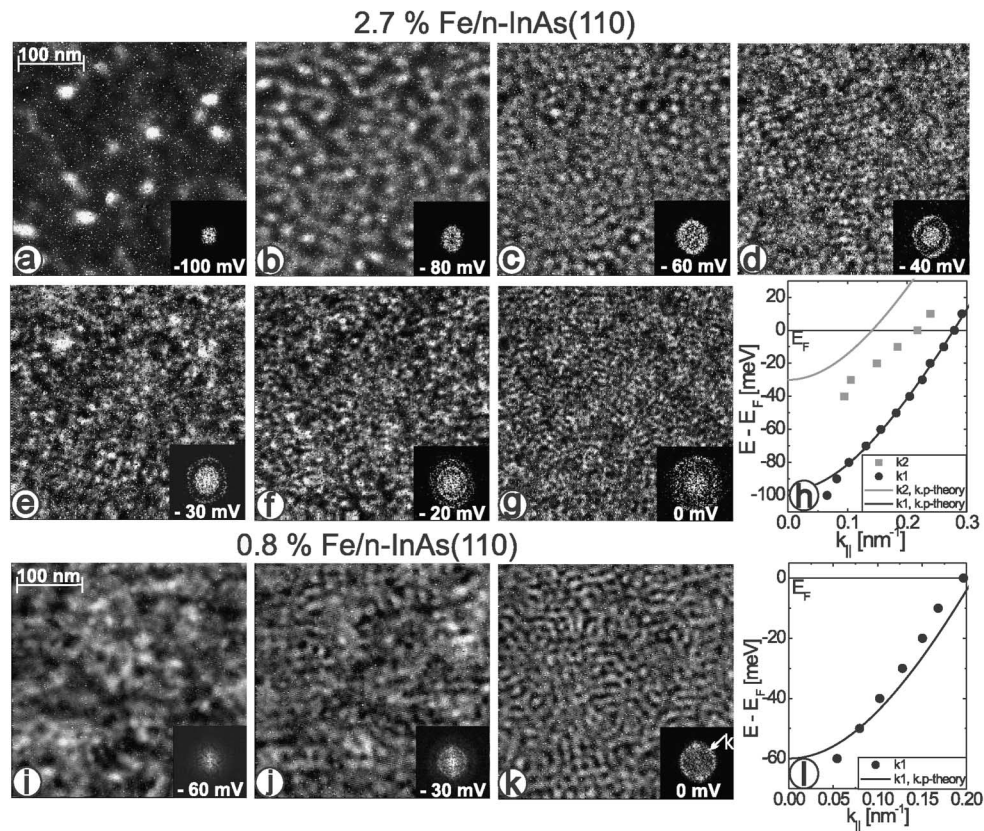

FIG. 3. (a)–(g) dI/dV images (LDOS images) of 2.7% Fe/n-InAs(110) at different V as indicated; $V_{stab} = 100$ mV, $I_{stab} = 300$ pA; bright spikes in the images are Fe atoms. Insets: Fourier transformations (FT) of dI/dV images. (h) Dominating k values corresponding to rings in FT's in comparison with dispersion curve of unperturbed InAs (lines) [16]. (i)–(l) Same as (a)–(h) but for 0.8% Fe/n-InAs(110); surface area belongs to the potential in Fig. 2(c).
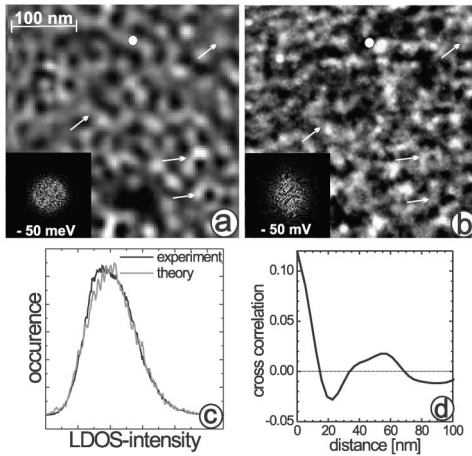
FIG. 4.   (a) LDOS calculated from the potential landscape in Fig. 2(c) [18]; $E = -50$ meV. (b) Normalized dI/dV image of the same area; $V = -50$ mV, $V_{stab} = 100$ mV, $I_{stab} = 300$ pA. Insets are FT's. Dots mark identical sample positions as deduced from constant current images. (c) Intensity distribution of the LDOS in (a) and (b); for the sake of comparison the experimental curve is stretched by 5%. (d) Cross correlation function between experimental and calculated image.

and potential and LDOS can be directly compared. This is a crucial result, since the known effective mass, potential landscape, and electron density completely determine the SE, and the output of the SE, the LDOS, is measured. In particular, it is used to show that the additional k values contributing to the LDOS are caused by the interaction of the electrons with the potential disorder. We solve the SE for noninteracting particles numerically using periodic boundary conditions, the measured disorder potential, and no adjustable fit parameter [18,19]. To construct the LDOS, the resulting squared wave functions are weighted with the known energy resolution of the experiment. The resulting LDOS for a particular energy is shown in Fig. 4(a) in comparison with the measured LDOS in Fig. 4(b). The correspondence is reasonable; i.e., several features as the central ring structure or other smaller structures marked by arrows appear in both images. The FT's (insets) and the intensity distributions of the LDOS [Fig. 4(c)] show very good agreement, demonstrating that the additional k values in the FT's and the strength of the corrugation are indeed caused by the interaction with the potential disorder. Figure 4(d) shows the cross correlation function between experimental and theoretical images. Oscillations on the length scale of the unperturbed electron wavelength are found, which demonstrates quantitatively the reasonable agreement between calculated and measured patterns.

In summary, we presented an experimental method to determine the potential landscape and the LDOS of the same disordered 2DES area. This is a decisive prerequisite for detailed studies of the 2DES LDOS under different conditions. The results obtained here are successfully interpreted in terms of mixing of different k states by the inhomogeneous potential landscape, which is evidenced by comparing the calculated LDOS using the measured potential landscape and the measured LDOS.

[1]   See, e.g., T. Ando *et al.*, Rev. Mod. Phys. **54**, 437 (1982); P. A. Lee *et al.*, Rev. Mod. Phys. **57**, 287 (1985).

[2]   E. Abrahams *et al.*, Phys. Rev. Lett. **42**, 673 (1979); K. v. Klitzing *et al.*, Phys. Rev. Lett. **45**, 494 (1980); D. C. Tsui *et al.*, Phys. Rev. Lett. **48**, 1559 (1982).

[3]   R. Joynt *et al.*, Phys. Rev. B **29**, 3303 (1984); B. Kramer *et al.*, Rep. Prog. Phys. **56**, 1469 (1993).

[4]   K. Kanisawa *et al.*, Phys. Rev. Lett. **86**, 3384 (2001).

[5]   2DES's in metals have been extensively studied, but the large electron density in these systems reduces the influence of disorder and interaction. M. F. Crommie *et al.*, Nature (London) **363**, 524 (1993); P. T. Sprunger *et al.*, Science **275**, 1764 (1997).

[6]   M. Morgenstern *et al.*, Phys. Rev. B **61**, 13 805 (2000).

[7]   N. B. Zhitenev *et al.*, Nature (London) **404**, 473 (2000); S. H. Tessmer *et al.*, Nature (London) **392**, 51 (1998); G. Finkelstein *et al.*, Science **289**, 90 (2000).

[8]   Chr. Wittneven *et al.*, Phys. Rev. Lett. **81**, 5616 (1998).

[9]   Chr. Wittneven *et al.*, Rev. Sci. Instrum. **68**, 3806 (1997).

[10]   K. Rossnagel *et al.*, Nucl. Instrum. Methods Phys. Res., Sect. A **467–468**, 1485 (2001).

[11]   R. Dombrowski *et al.*, Phys. Rev. B **59**, 8043 (1999); M. Morgenstern *et al.*, J. Electron Spectrosc. Relat. Phenom. **109**, 127 (2000).

[12]   LDOS and dI/dV coincide as long as V is small [11] and electron-electron interactions are negligible.

[13]   The number of electrons donated is the product $n \cdot A$ with A being the image area and $n = \sum_i \int_{E_i}^{E_F} \frac{m_{eff}}{\pi \hbar^2} dE$ the electron density of the 2DES.

[14]   K. Hirakawa *et al.*, Phys. Rev. B **33**, 8291 (1986).

[15]   The number of contributing states $\overline{N}$ is the product of 2DES DOS $= \frac{m_{eff}}{\pi \hbar}$, image size A, and energy resolution ΔE. It is $\overline{N} = 30$ for each subband; i.e., $\overline{N} = 30$ for $V \leq -30$ mV and $\overline{N} = 60$ for $V \geq -30$ mV.

[16]   U. Merkt *et al.*, Phys. Rev. B **35**, 2460 (1987).

[17]   The experimental noise is considerably smaller than the intensities depicted in the FT's.

[18]   C. Metzner *et al.*, Phys. Rev. B **58**, 7188 (1996).

[19]   The contributing energy scales are roughly given by the average kinetic energy $E_{kin} = 30$ meV, the σ value of the potential fluctuations $\sigma(V) = 5$ meV, and the electron-electron repulsion of regularly distributed point charges $E_{Coul} = 5$ meV indicating that, away from E_F, electron-electron interactions can be neglected.